

Calculation of Aircraft Wake Velocity Profiles and Comparison with Experimental Measurements

Coleman duP. Donaldson,* Richard S. Snedeker,† and Roger D. Sullivan‡
Aeronautical Research Associates of Princeton, Inc., Princeton, N.J.

A method is developed for the calculation of the initial inviscid form of rolled-up wake vortices behind a wing having arbitrary lift distribution. The method makes use of the Betz assumptions of conservation of wake vorticity and moments of vorticity. It is found that a simple relationship exists between the radial distribution of vorticity in the rolled-up wake and the spanwise lift distribution. Computed tangential velocity profiles for DC-7, DC-9, and C-141 aircraft are shown to compare favorably with profiles measured by the FAA during tower flyby tests of these aircraft in both flapped and unflapped configurations.

Nomenclature

A	= point of division between tip and flap shed vorticity
B	= point of division between flap and fuselage shed vorticity
b	= wingspan
C	= point denoting centerline boundary of shed vorticity
d_c	= diameter of vortex core
P	= point on load curve
R	= radius within which shed vorticity from one-half the wing rolls up
r	= radial coordinate
U_{IND}	= total horizontal component of induced velocities from opposite vortex and both image vortices
U_w	= wind velocity parallel to ground
U'	= $(V_{\theta'}^2 - V_{IND}^2)^{1/2}$
V_{IND}	= total vertical component of induced velocities from opposite vortex and both image vortices
$V_{\theta'}$	= resultant mean velocity to which a sensor responds
v	= tangential velocity in vortex
y	= spanwise coordinate
y_m	= spanwise location of a local maximum of shed vorticity distribution
y^*	= point denoting subtangent of point P
\bar{y}	= spanwise location of centroid of shed vorticity distribution
\bar{y}_f	= spanwise location of centroid of shed vorticity for flap vortex
\bar{y}_t	= spanwise location of centroid of shed vorticity for tip vortex
Γ	= circulation of wing
Γ'	= circulation of rolled-up vortex
Γ_f	= circulation of flap vortex
Γ_t	= circulation of tip vortex
Γ_0	= total circulation
δ_f	= flap deflection
η	= dummy variable for y
θ	= circumferential coordinate
ρ	= dummy variable for r

I. Introduction

UNTIL quite recently, the analysis of aircraft wakes has frequently depended upon the simplified model of vortex roll-up made popular by Spreiter and Sacks.¹ It has be-

Presented as Paper 74-39 at the AIAA 12th Aerospace Sciences Meeting, Washington, D.C., January 30–February 1, 1974; submitted February 8, 1974, revision received May 7, 1974. This work was sponsored by the Department of Transportation, Federal Aviation Administration, and the Air Force Office of Scientific Research. The authors wish to thank the following individuals and organizations for their cooperation and assistance in providing the required aircraft loading data and experimental results: O. R. Dunn and J. A. Thelander, Douglas Aircraft Company; J. G. Theisen and J. J. Cornish III, Lockheed-Georgia Company; and L. J. Garodz and N. Miller, FAA-NAFEC.

Index categories: Aircraft Aerodynamics (Including Component Aerodynamics); Jets, Wakes, and Viscid-Inviscid Flow Interactions.

*President, Associate Fellow AIAA.

†Associate Consultant, Member AIAA.

‡Vice President and Senior Consultant, Member AIAA.

come increasingly evident, however, as new experimental wake measurements have accumulated, that a more accurate method is required to explain the data adequately. In 1971, Donaldson² demonstrated that the method first suggested by Betz³ in 1932 gives a considerably more accurate description of the radial distributions of vorticity and tangential velocity in rolled-up vortices than that given by other methods. The basic idea of the Betz method is the replacement of the difficult computation of the precise details of the inviscid roll-up of the vortex sheet with a local axisymmetric distribution of vorticity, so constituted and so located that proper consideration is given to the conservation of vorticity and moments of vorticity behind each half of the wing.

For elliptic and near elliptic load distributions, the Betz theory gives an excellent description of the initial inviscid trailing vortex pattern produced by a wing. Unfortunately, in the vicinity of airports, where the problem of wake encounter is most prevalent, the large aircraft which produce the strongest wakes usually operate with some degree of flap deflection. Under these conditions, the spanwise load distributions may be quite complex so that the original form of the Betz analysis is no longer appropriate. In this paper, therefore, we shall extend the Betz method to the case of flapped wings and present a general recipe for evaluating the initial character of the wake. In addition, we shall compare the tangential velocity profiles calculated by this method with experimental measurements made by the Federal Aviation Administration in the wakes of several large transport aircraft.

II. Betz Method and Its Extension to Complex Load Distributions

Several investigators have attempted to calculate in detail the roll-up of the wake behind a wing.^{4–6} This is a complex calculation, and most investigators have found great difficulty in carrying the calculation out to long times because of the inherent instabilities in these calculations. In 1932, Betz³ gave a formula for approximating the completely rolled-up character of the wake with an application to a wing with an elliptic load distribution. Considering a station far enough downstream that the roll-up could be considered complete, Betz proposed that the distribution of vorticity for each half of the wing might be considered axisymmetric about a center of roll-up.

Quantitatively, the theory relates the wing loading Γ , a function of the spanwise station y , to the circulation in the rolled-up vortex Γ' as a function of radial distance from the center of the vortex r . The derivative $d\Gamma/dy$ is loosely referred to as the vorticity shed by the wing. (Ac-

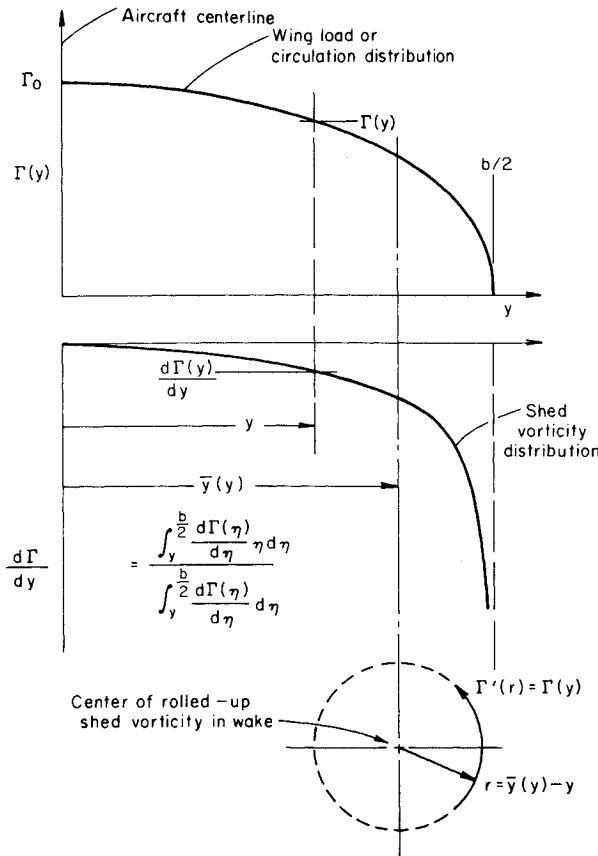


Fig. 1 Illustration of the Betz roll-up model for a simply loaded wing.

tually, it is the strength of the vortex sheet; $-d\Gamma/dy$ is the integral of the vorticity through the thickness of the vortex sheet.) In the rolled-up vortex, $d\Gamma'/dr$ is the integral of the vorticity around a circle of radius r . Betz proposed that the following invariants of the roll-up process be preserved:

$$-\int_0^{b/2} \frac{d\Gamma(y)}{dy} dy = \int_0^R \frac{d\Gamma'(r)}{dr} dr = \Gamma_0 \quad (1)$$

$$-\int_0^{b/2} \frac{d\Gamma(y)}{dy} y dy = \Gamma_0 \bar{y}_t \quad (2)$$

$$-\int_0^{b/2} \frac{d\Gamma(y)}{dy} (y - \bar{y}_t)^2 dy = \int_0^R \frac{d\Gamma'(r)}{dr} r^2 dr \quad (3)$$

where b is the wing span and R is the radius (not known a priori) within which the vorticity from each half of the wing is rolled up. Γ_0 , the circulation at the centerline of the wing and y_t , the centroid of the shed vorticity of the complete half-wing, are defined by Eqs. (1) and (2).

Furthermore, Betz stipulated that the roll up satisfy these invariants from the inside according to the following scheme:

$$-\int_y^{b/2} \frac{d\Gamma(\eta)}{d\eta} d\eta = \int_0^r \frac{d\Gamma'(\rho)}{d\rho} d\rho = \Gamma(y) \quad (4)$$

$$\int_y^{b/2} \frac{d\Gamma(\eta)}{d\eta} \eta d\eta = \bar{y}(y) \int_y^{b/2} \frac{d\Gamma(\eta)}{d\eta} d\eta \quad (5)$$

$$-\int_y^{b/2} \frac{d\Gamma(\eta)}{d\eta} [\eta - \bar{y}(y)]^2 d\eta = \int_0^r \rho^2 \frac{d\Gamma'(\rho)}{d\rho} d\rho \quad (6)$$

In these equations, η and ρ are dummy variables for y

and r , respectively. It is easy to see from Eq. (5) that $\bar{y}(y)$ is the spanwise location of the centroid of the vorticity shed by the wing outboard of the spanwise location y . The relationships are illustrated in Fig. 1.

By following these rules, Betz gave a rather complicated implicit expression for the distribution $\Gamma'(r)$ for the case of an elliptically loaded wing. More recently, Brown⁷ has given results for a parabolically loaded wing, and Mason and Marchman⁸ have given results for unswept wings of various tapers and twists.

The description can be simplified by performing the following steps. Differentiating Eq. (4) with respect to r , one obtains

$$\frac{d\Gamma}{dy} \frac{dy}{dr} = \frac{d\Gamma'}{dr} \quad (7)$$

Differentiation of Eq. (6) with respect to r yields

$$[y - \bar{y}(y)]^2 \frac{d\Gamma}{dy} \frac{dy}{dr} = r^2 \frac{d\Gamma'}{dr} \quad (8)$$

since the term involving $d\bar{y}/dr$ drops out by virtue of (5). Substituting Eq. (7) into Eq. (8) results in

$$(y - \bar{y})^2 = r^2 \quad (9)$$

or, since $\bar{y} > y$,

$$r = \bar{y} - y \quad (10)$$

This result has been obtained independently by Rossow⁹ and Jordan.¹⁰ Since Eq. (4) can be integrated to obtain

$$\Gamma(y) = \Gamma'(r) \quad (11)$$

Eq. (10) states that the radius from the center of roll-up at which one finds the circulation equal to the circulation at the spanwise location y on the wing is equal to the distance from y to the centroid of the shed vorticity outboard of y .

If Betz' recipe is followed exactly for the case of wings having load distributions which are complex, such as those found on wings with flaps and spoilers extended, one finds an immediate difficulty, namely that r becomes a multiple-valued function of y . This may be illustrated by calculating the derivative dr/dy of Eq. (10),

$$\frac{dr}{dy} = \frac{d\bar{y}}{dy} - 1 \quad (12)$$

An expression for $d\bar{y}/dy$ can be obtained from Eqs. (4) and (5), which, after some manipulation, give

$$\frac{d\bar{y}}{dy} = -\frac{\bar{y} - y}{\Gamma} \frac{d\Gamma}{dy} \quad (13)$$

Substitution of this expression into Eq. (12) gives, finally,

$$\frac{dr}{dy} = -\frac{\bar{y} - y}{\Gamma} \frac{d\Gamma}{dy} - 1 \quad (14)$$

Now, according to our formulation, the vorticity from the tip of the wing $y = b/2$, appears at $r = 0$. Thus, to have a conventional roll-up, we wish to find that as y decreases, r increases; i.e., a conventional roll-up is possible if dr/dy is always negative. If the condition $dr/dy = 0$ occurs in an attempted roll-up calculation, this means that the circulation is becoming multivalued at a given point r . Since this is impossible, it is clear that a single vortex roll-up according to Betz is impossible.

From the above discussion, it is evident that for a load distribution such as that shown in Fig. 2, we may not proceed with the calculation of the roll-up of a single tip vortex much inboard of the point P , for as one does, one quickly runs into a singular behavior of the vortex. It can be shown that this behavior is equivalent to having point y^* move inboard of point $\bar{y}(y)$.

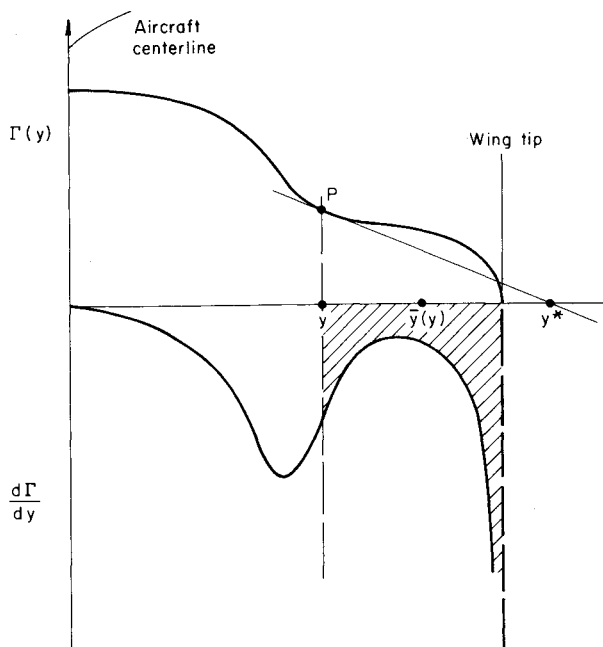


Fig. 2 Representative load distribution on a flapped wing $\Gamma(y)$, upper curve, and distribution of shed vorticity $d\Gamma/dy$ from same wing, lower curve.

Before discussing how such multiple vortex roll-up might be calculated, let us make an observation about the velocity $v(0)$ at the center of a tip vortex. It is a consequence of Eqs. (11) and (14) together with the inviscid vortex solution $v(r) = \Gamma'(r)/2\pi r$ that

$$v(0) = -\frac{1}{\pi} \left(\frac{d\Gamma}{dy} \right)_{b/2} \quad (15)$$

Thus, the exact behavior of the load at the tip has a profound effect on the inviscid roll-up of a vortex. By changing the load distribution just slightly so as to reduce $d\Gamma/dy$ at the tip, the maximum velocities that can be achieved in roll-up can be reduced accordingly.

We may now turn to the problem of multiple vortex formation. Consider the load distribution shown in Fig. 3. In order to eliminate the singular behavior of vortex roll-up just discussed, we will divide up the shed vorticity from the wing in the following way: We consider the distribution of the absolute value of the shed vorticity $|d\Gamma/dy|$. Let us consider the points where this function is a minimum. For the case considered in Fig. 3, these points are A , B , and C . We now assume that all the vorticity shed outboard of the point A will roll up into a "tip" vortex, that all the vorticity shed between the points A and B will roll up into a second vortex that we will generally call the "flap" vortex, and that all the vorticity shed between B and C will roll up into a third vortex that we will generally call the "fuselage" vortex. Actually, any number of vortices might be found by following the procedure of dividing the vorticity up according to where the minima of $|d\Gamma/dy|$ occurred. In an analysis of the initial deformation of the vortex sheet for load distributions of this kind, Yates¹¹ has confirmed that this method of apportioning the shed vorticity is quite accurate. He has also found that the centers of roll-up are located very near to those found by the present method.

Now we wish to roll up the vorticity shed from the wing so that the Betz invariants are preserved in the process. This may be accomplished if, for each of the three regions of shed vorticity that we have just defined, we roll all the vorticity in each region up about its own centroid in such a way that the moment of inertia of each section of shed

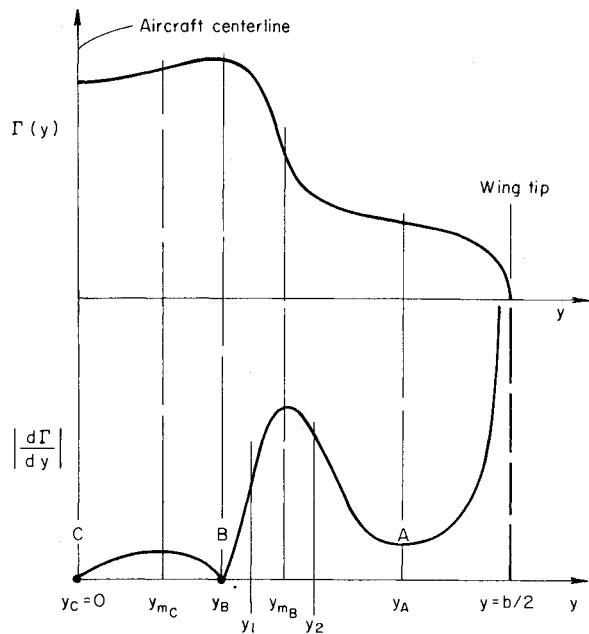


Fig. 3 Load distribution which will produce three vortices.

vorticity is preserved about this centroid. As an example, consider the vorticity shed between the points A and B of Fig. 3. Let us call this vortex B . We will roll the vorticity shed from the wing in the region $A-B$ into a vortex located at the centroid \bar{y}_B of the shed vorticity for this region. This position is defined by

$$\bar{y}_B \int_{y_B}^{y_A} \frac{d\Gamma}{dy} dy = \int_{y_B}^{y_A} y \frac{d\Gamma}{dy} dy \quad (16)$$

We assume, as before, that the Betz invariants are preserved in detail. To write expressions for this detailed preservation that are equivalent to Eqs. (4-6) we must decide what part of the vorticity shed between A and B is rolled up into the center of the vortex. It seems reasonable to assume that the most intense region of vorticity shedding will wind up at the center of the vortex. Let y_{mB} be the position of the maximum of $|d\Gamma/dy|$ between B and A . The detailed Betz invariants that we desire can now be written

$$-\int_{y_1}^{y_2} \frac{d\Gamma}{dy} dy = \int_0^{r_B} \frac{d\Gamma_B'}{dr} dr \quad (17)$$

and

$$-\int_{y_1}^{y_2} \frac{d\Gamma}{dy} (y - \bar{y}_{12})^2 dy = \int_0^{r_B} r^2 \frac{d\Gamma_B'}{dr} dr \quad (18)$$

where y_1 and y_2 are arbitrary points inboard and outboard of y_{mB} , and \bar{y}_{12} is the centroid of the shed vorticity between y_1 and y_2 , namely

$$\bar{y}_{12} \int_{y_1}^{y_2} \frac{d\Gamma}{dy} dy = \int_{y_1}^{y_2} y \frac{d\Gamma}{dy} dy \quad (19)$$

An expression for the radius at which one would find the circulation $\Gamma_B'(r_B)$ equal to $\Gamma(y_1) - \Gamma(y_2)$ can be derived from Eqs. (17) and (18). Thus, we find

$$r_B^2 = \frac{(y_1 - \bar{y}_{12})^2 \frac{d\Gamma_1}{dy} \frac{dy_1}{dr_B} - (y_2 - \bar{y}_{12})^2 \frac{d\Gamma_2}{dy} \frac{dy_2}{dr_B}}{\frac{d\Gamma_1}{dy} \frac{dy_1}{dr_B} - \frac{d\Gamma_2}{dy} \frac{dy_2}{dr_B}} \quad (20)$$

However, the distribution of circulation is not fixed unless we prescribe a relationship between y_1 and y_2 . The rela-

tionship which gives the simplest expression for the roll-up and one which is equivalent to that found by Betz for tip roll-up is

$$(y_2 - \bar{y}_{12})^2 = (y_1 - \bar{y}_{12})^2 \quad (21)$$

That is, one chooses y_1 and y_2 in such a way that they are always equidistant from the centroid of shed vorticity between y_1 and y_2 . Putting Eq. (21) into (20) results in

$$r_B^2 = (y_2 - \bar{y}_{12})^2 = (y_1 - \bar{y}_{12})^2 \quad (22)$$

or

$$r_B = y_2 - \bar{y}_{12} = \bar{y}_{12} - y_1 \quad (23)$$

Here, the similarity of this result and the result for tip roll-up, Eq. (10), is obvious. Now Eq. (17) may be written

$$\Gamma_B'(r_B) = \Gamma(y_1) - \Gamma(y_2) = \Gamma_1 - \Gamma_2 \quad (24)$$

and Eq. (19) may be written

$$\bar{y}_{12} = \frac{\int_{y_1}^{y_2} y \frac{d\Gamma}{dy} dy}{\Gamma_2 - \Gamma_1} \quad (25)$$

We may, therefore, take Eqs. (23-25) as a new recipe for computing the roll-up of vorticity between any two minima of $|d\Gamma/dy|$ on a wing. These formulas hold so long as y_1 remains greater than y_B , and y_2 remains less than y_A (see Fig. 3). If y_2 reaches y_A before y_1 reaches y_B , the roll-up may be continued by holding y_2 and, hence, Γ_2 fixed and proceeding with the roll-up, letting $r = \bar{y}_{12} - y_1$ until y_1 reaches y_B . If y_1 reaches y_B before y_2 reaches y_A , then the roll-up is continued holding y_1 and, hence, Γ_1 fixed and letting $r = y_2 - \bar{y}_{12}$.

It should be clear that the prescription given above for calculating what might be a centralized roll-up for each segment of vorticity shed from a wing can be applied to any number of vortex segments. The method should be applied for the tip vortex if the maximum shedding of vorticity appears inboard of the tip. It is obvious that it will reduce to the classical Betz description if the maximum shedding does indeed appear at the tip.

Before going on to describe some of the consequences of calculating roll-up in the manner just described and com-

paring results of computations with experimental results, we note that it is a consequence of Eq. (23) and the inviscid vortex solution that

$$v(0) = -\frac{1}{\pi} \left(\frac{d\Gamma}{dy} \right)_{y=y_m} \quad (26)$$

As in the case of the tip vortex, we see that the velocities near the center of a "flap" or inboard vortex are not related to the strength of the vortex but are merely a manifestation of the rate of change of load on the wing near the end of the flaps.

III. Comments on Vortex Roll-Up

The method just given for approximating the character of the vortices that might be shed by a flapped wing can be helpful in understanding trailing vortex behavior, but it does not give a complete description of an actual roll-up. Indeed, in an actual wake, any concentrations or centers of vorticity shed by the wing move relative to one another in accordance with the velocities that these centers induce in each other. A general tendency when two closely spaced vortices are shed from each half of a wing is for these vortices to rotate about one another on each side so as to preserve the moment of the shed vorticity. Such a condition may be observed experimentally on a straight wing with flaps extending to, say, 75% or more of the semi-span. This type of behavior is shown in Fig. 4a. The centers of vorticity shed from each side tend to spiral about their common centroid, as this centroid moves downward behind the wing in the velocity field induced by the two vortices from the opposite tip. In such cases, it has generally been found that the two vortices on each side remain in rather intimate contact with each other and, eventually, these regions of vorticity of equal size diffuse into each other.

For flap semispans that are of the order of 50% or less, another type of vortex behavior can be observed. In this case, the centers of vorticity shed by each side of the wing are not too close together, and the tip vortex moving in the velocity field induced by the flap vortex moves up above the wing and towards the plane of lateral symmetry of the aircraft. The flap vortex moves down and outward. This behavior of the shed vortices is shown in Fig. 4b. In this case, after a short while, the two tip vortices, which are of opposite sign, come into close proximity. They are thus able to interact with one another and, as such interactions are unstable, they may be able to loop off or explode and greatly modify one another. This modification by instability can proceed quite rapidly because of the small separations that are achieved between the two vortices of opposite sign. If such an interaction were to result in the effective cancellation of these two vortices, the two remaining vortices would have to move further apart in order to conserve the moment of the shed vorticity. This disturbance might then excite an inviscid instability of these remaining vortices.

Although the prescription for computing vortices given in the previous section does not explicitly treat these relative motions of vortices, one can obtain from calculations of the type suggested the parameters required to determine the type of motion that is to be expected behind the wing. It should be pointed out that the two types of vortex behavior discussed above are but two of a large variety of types of vortex motion that can be observed behind a wing. These motions depend upon the number of centers of vorticity shed by each half of the wing and their relative strengths and spacing. Since the present method enables one to calculate these quantities, it should, if it is experimentally verified, enable one to classify the type of vortex wake with which one is dealing. Such information

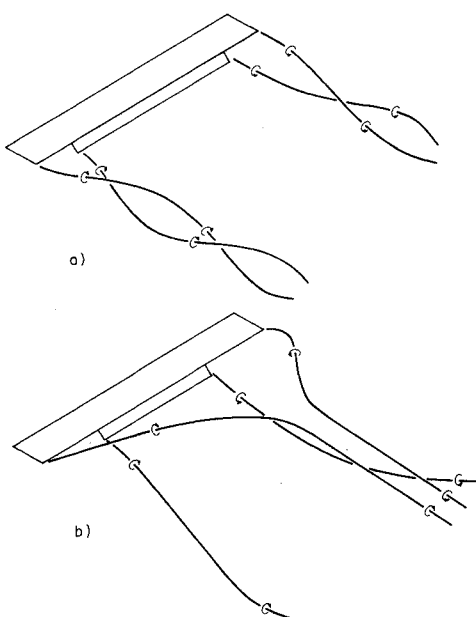


Fig. 4 Behavior of the tip and flap vortex for a) large-percentage-span flaps and b) small-percentage-span flaps at moderate lift coefficients and flap deflections.

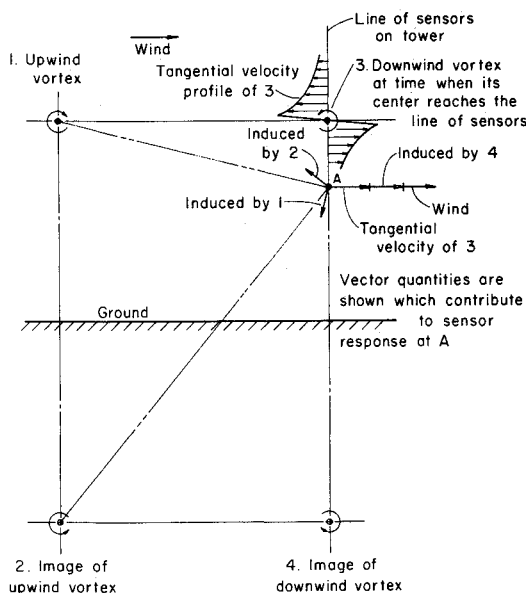


Fig. 5 Diagram showing the wake vortex system at the time the center of the downwind vortex reaches the line of sensors.

is essential if one is to determine the eventual dissipation of the wake of an aircraft.⁸

Another aspect of wake roll-up that is not treated herein is the effect of wing profile drag or the effect of wing-mounted propulsion systems. The inclusion of profile drag in the specification of the shed vortices can, in all probability, be handled by an extension of the method developed by Brown⁷ for a tip vortex roll-up according to the Betz method. Recently, Bilanin¹² has undertaken to make a more rigorous analysis of this problem. Although the inclusion of the effects of propulsion systems is far more complicated, it is clear that the location of the centerline of engine thrust and the disc loading of the thrusting devices relative to dynamic pressure are most important parameters. We certainly would expect a large effect of jet engine thrust on the behavior of a wake in the vicinity of an airplane if the thrust centerline happened to coincide, or nearly coincide, with the center of roll-up of, say, the flap vortex of an airplane in landing configuration.

IV. Comparison of Computed and Measured Vortex Velocity Profiles

It has been suggested that the character of a wake which is made up of one or more rolled-up vortex pairs may be determined by considering the initial roll-up process to be inviscid. Application of the Betz conservation relations to a known spanwise distribution of circulation Γ for a particular aircraft in a particular flight condition then permits one to calculate the distribution of tangential velocity which might be found in the wake vortices. The agreement between profiles calculated by this method and those measured experimentally would be expected to depend not only on the limitations inherent in the method, but on the effects of instability and aging as well. These latter effects are implicit in any measurements taken at some time after roll-up is complete. During this time, ambient or aircraft-generated turbulence, wind gusts, and distortion due to mutual interaction and diffusion would all contribute in some degree to the aging process. In this section, a comparison will be made between

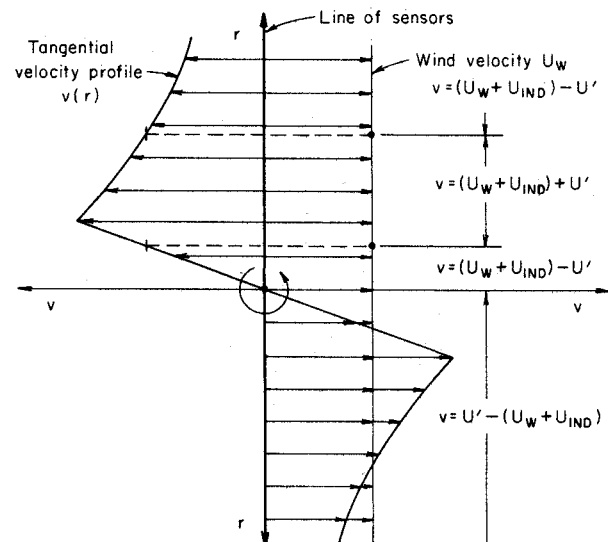
§Of the two types of wake behavior previously discussed, it is not known at this time which would result in the faster dissipation of the wake. This is surely the topic of a worthwhile investigation.

velocity profiles computed by the Betz method and those measured during full-scale flight tests of several aircraft.

NAFEC Full-Scale Vortex Measurements

The data which are used as a basis for comparison in this study were selected from the results of full-scale tower flyby tests carried out by the Federal Aviation Administration at the National Aviation Facilities Experimental Center at Atlantic City, N.J.

The NAFEC test technique¹³ consists in the measurement of vortex tangential velocity profiles in the wake of an aircraft which flies by to the windward side of an instrumented tower. Instrumentation consists of hot film sensors mounted on the tower at closely spaced vertical intervals. Tangential velocity profiles in the vortices are deduced from the recorded time histories of the sensor signals. In the data reduction method used in this study,¹⁴ corrections were made for the induced effects of the opposite vortex, as well as the ground plane images of both vortices. The system as applied to the downwind vortex is illustrated in Fig. 5. For cases in which more than one vortex concentration might be expected behind each half of the wing, this simple system might appear to be too limited. However, the experimental data indicate that, at the time of intercept, a single vortex concentration is, indeed, dominant. It may be surmised, following the discussion of Sec. III, that other concentrations which may form initially either have been distorted as they interact with the dominant vortex and have become diffused in the region surrounding it or have left the immediate vicinity of the dominant vortex so that their presence would not be observed in this type of test. The total circulation of such a vorticity concentration would still be equal to the total for the complete half wing, but the recognizable part of



At a given sensor, the resultant velocity to which the sensor responds is

$$V_\theta = \sqrt{(U_w + U_{IND} \pm v)^2 + V_{IND}^2}$$

where U_w = wind velocity parallel to ground

U_{IND} = total horizontal component of induced velocities from upwind vortex and both images

v = local tangential velocity in vortex

V_{IND} = total vertical component of induced velocities from upwind vortex and its image

In the formulas above,

$$U' = \sqrt{V_\theta^2 - V_{IND}^2}$$

Fig. 6 Data reduction relations for downwind vortex.

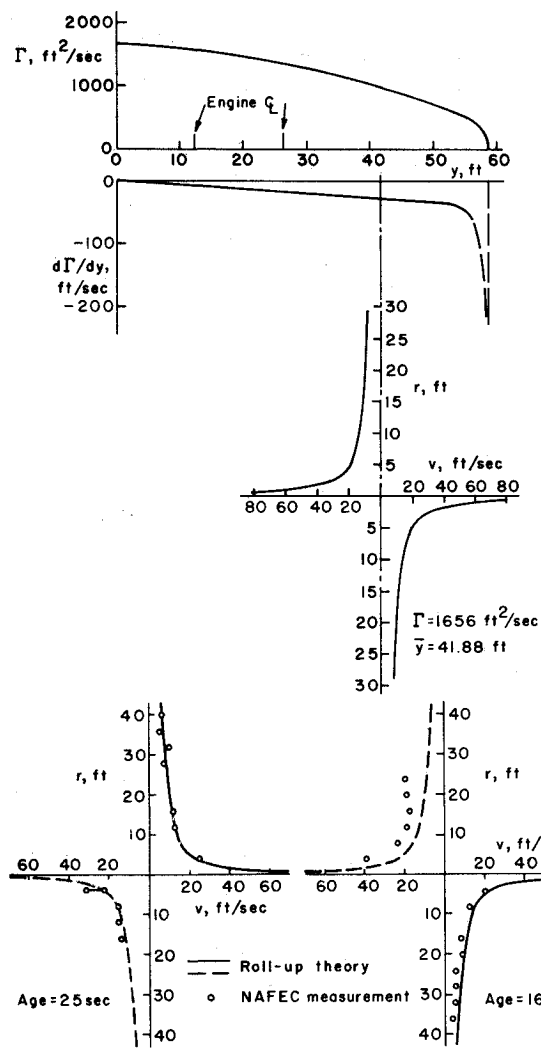


Fig. 7 Spanwise distributions of Γ and $d\Gamma/dy$ and the radial distributions of tangential velocity for vortices in the wake of a DC-7 in holding configuration.

the tangential velocity profile would be that of the dominant vortex alone.

The way in which the tangential velocities are determined from the sensor output data for different portions of the vortex is shown in Fig. 6 for the downwind vortex. To properly apply the relations given, it is necessary to identify the points where the magnitudes of the quantities U' and $U_w \pm U_{IND}$ become equal. Two such "null" points can occur for a typical vortex velocity profile: one inside the core and one outside the core. For the downwind vortex, these points lie above the centerline; for the upwind vortex, they lie below. In working with the NAFEC data, it was sometimes difficult to identify these points with certainty. Since the profile on the opposite side of the centerline was usually well defined, however, this difficulty was not a serious problem.

Computation of Load Distributions and Velocity Profiles

The computation of the initial profile of tangential velocity in a rolled-up vortex by the method described in Sec. II requires that the spanwise circulation distribution $\Gamma(y)$ be known. For the aircraft used in this study, information was obtained from the manufacturers which made possible the computation of the desired distributions.

Two computer programs were developed at ARAP. to enable the computation of the tangential velocity profiles from these load distributions. The first program computes

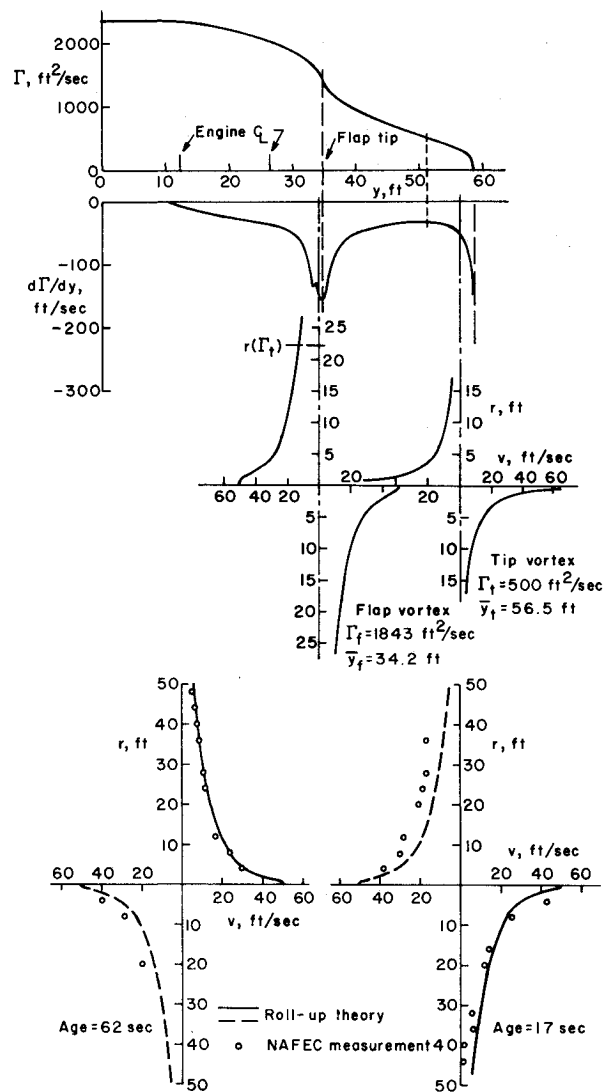


Fig. 8 Spanwise distributions of Γ and $d\Gamma/dy$ and the radial distributions of tangential velocity for vortices in the wake of a DC-7 in takeoff ($\delta_f = 20^\circ$) configuration.

the distribution $\Gamma(y)$ for a specific flight using a value of aircraft C_L calculated from flight parameters supplied by NAFEC. This distribution is then used to compute the profile $v(r)$ and the center of roll-up $\bar{y}(y)$ for the case of tip vortex roll-up as given by Eqs. (4-6). The second program is used to compute the profile $v(r)$ and center of roll-up $\bar{y}(y)$ for a flap vortex in accordance with Eqs. (17-19).

Comparison of Measured and Computed Profiles

Examples of the measured and computed tangential velocity profiles for DC-7, DC-9, and C-141 aircraft are presented in Fig. 7-11. The upper part of each figure shows the computed load distribution $\Gamma(y)$, the computed distribution of $d\Gamma/dy$, and the computed tangential velocity profile for the tip vortex and/or the flap vortex. The vortex is shown centered at the computed center of roll-up \bar{y} . The lower part of each figure shows the comparison of measured and computed tangential velocity profiles for both the upwind (left) and downwind (right) vortices. The computed profiles are plotted as solid lines on the side of the vortex centerline for which the vortex velocity is towards the tower. On the opposite side of the center, the measurements revealed a kind of "offset" effect which may have been due to probe interference in regions where

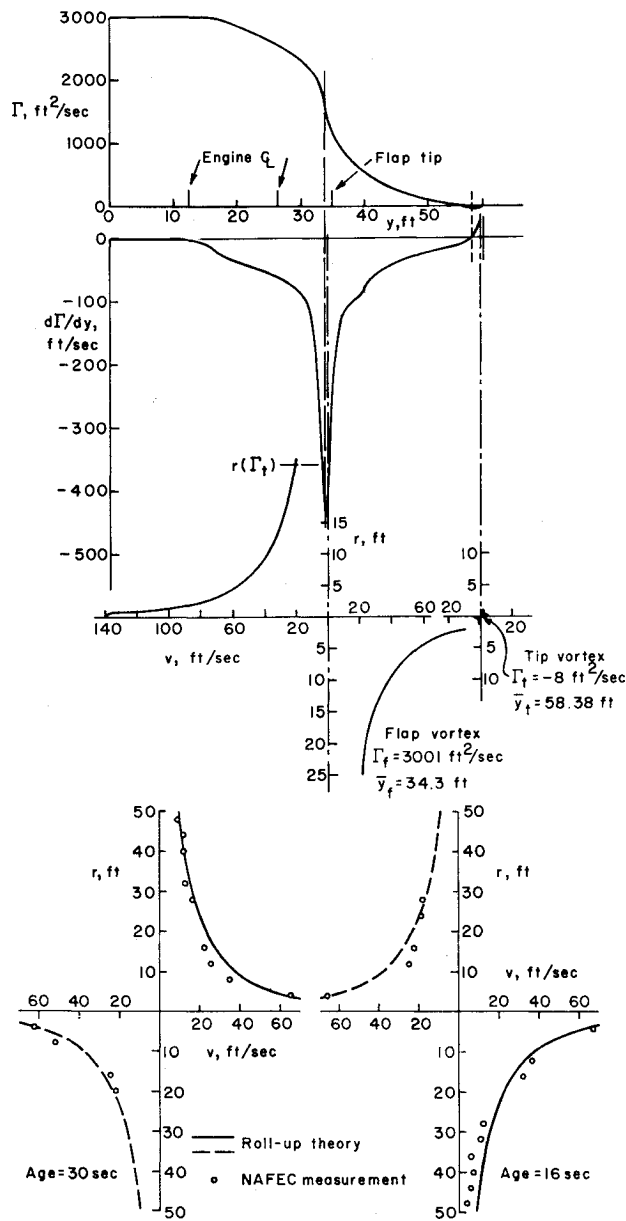


Fig. 9 Spanwise distributions of Γ and $d\Gamma/dy$ and the radial distributions of tangential velocity for vortices in the wake of a DC-7 in landing ($\delta_f = 50^\circ$) configuration.

the sensors were subject to net velocities away from the tower. For this region, the computed profile is plotted as a dashed line. For the flapped configurations (takeoff and landing), the computed profile shown is that of the flap vortex, this being the stronger and presumably dominant one in every case.

On the whole, the agreement between measurement and theory is quite satisfactory for all the aircraft in all configurations. This is so in spite of the wide differences in the detailed flowfields of the wings of these aircraft, each of which represents a distinct design class. The five cases shown here were selected from a total of 25 which were analyzed in detail. The remainder are given in Ref. 14. The 25 cases were, in turn, chosen out of a total of 199 which were made available by NAFEC. The choices were made on the basis of careful screening that eliminated data sets which were less complete or which exhibited ambiguity due to such factors as high ambient winds, gustiness, and apparent instrumentation problems. For all but four or five of the cases analyzed the quality of agreement between theory and measurement is similar to that shown here. In some of the remaining cases, the profile

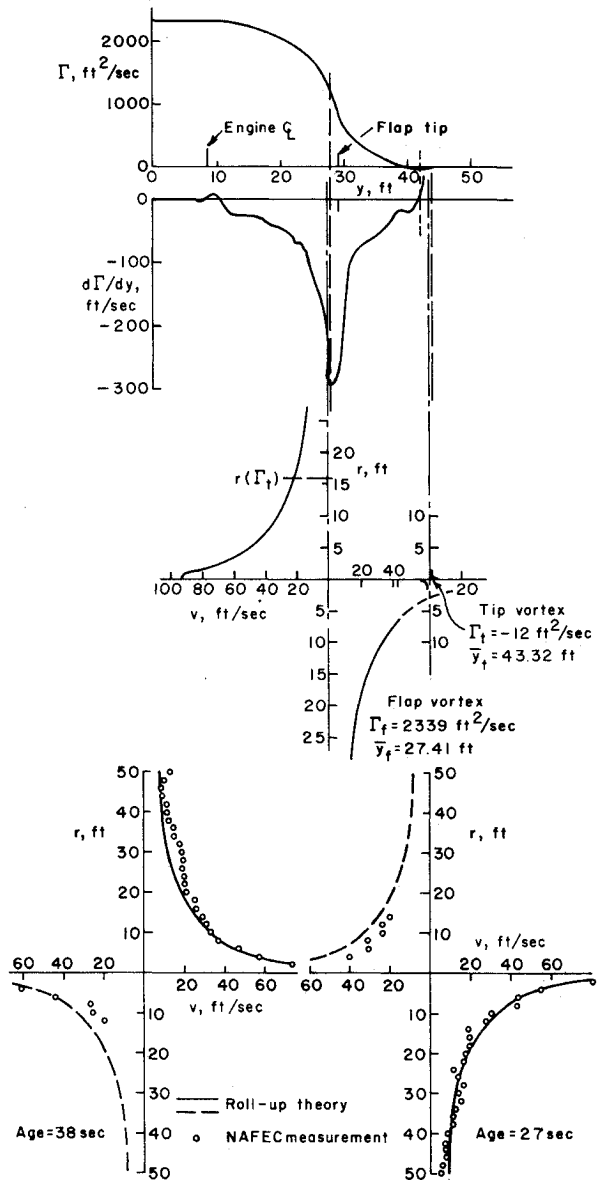


Fig. 10 Spanwise distributions of Γ and $d\Gamma/dy$ and the radial distributions of tangential velocity for vortices in the wake of a DC-9 in landing ($\delta_f = 50^\circ$) configuration.

shapes agree well, but the correction for wind velocity is apparently off enough to displace all of the data points relative to the estimated axis of symmetry. In other cases, one of the vortices of the pair showed better agreement than the other.

DC-7

For the tests with this aircraft, the NAFEC tower was instrumented with sensors spaced four feet apart (see Figs. 7-9). Therefore, the resolution of vortex structural details, such as the viscous core size, was more limited than for the later tests with one-foot sensor spacing. Nevertheless, it can be concluded from the data shown that the measured profiles for all three flight configurations match very closely the inviscid profiles computed by the present method. Furthermore, this match was found to hold true regardless of vortex age up to 62 sec.

DC-9

For this aircraft, the sensor spacing on the tower was one foot (Fig. 10). With its fuselage mounted engines, the DC-9 is representative of the "clean wing" jet design.

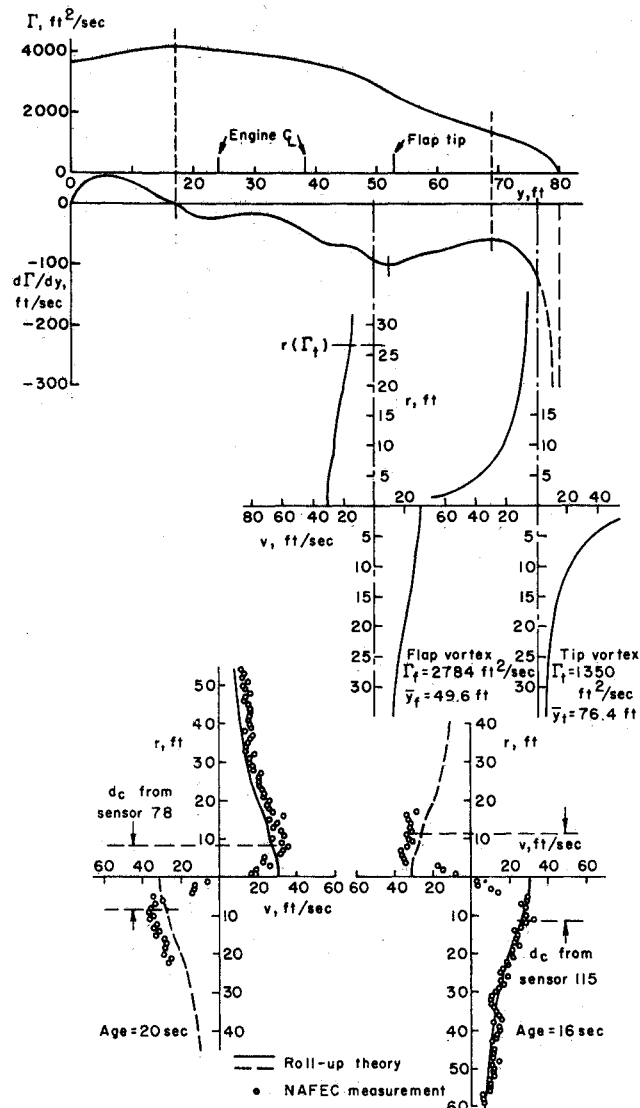


Fig. 11 Spanwise distributions of Γ and $d\Gamma/dy$ and the radial distributions of tangential velocity for vortices in the wake of a C-141 in takeoff ($\delta = 31^\circ$) configuration.

Thus it might be expected that effects on vortex roll-up due to engine exhausts or slipstreams would be absent. Although the exact nature of such influences is uncertain, it is apparent from the data that quite small vortex cores are possible with wings of this design. For both takeoff and landing configurations, the core diameters were found to be no greater than three or four feet. The computed profiles agree quite well with the data for distances of from one or two feet from the center outward. There is no apparent aging of these vortices for observation times of up to 38.6 sec.

C-141

Once again, the sensor spacing was one foot (Fig. 11). For this aircraft, too, the agreement between the profiles computed by the inviscid method and those measured during flyby is quite satisfactory. For the takeoff configuration shown, the computed profiles are quite flat, with tangential velocities of 10 fpm as far as 50 ft from the vortex centerline. It is also significant that the inviscid computation for this Γ distribution results in relatively low tangential velocities near the center [cf. Eq. (26)]. The data for these cases fall quite close to the computed profiles except in the central region. Here there is definite

experimental evidence of core penetration by a substantial number of sensors. Core diameter d_c estimates for the vortices shown range from 16-26 ft. The presence of such cores can be verified by examining the time history of the sensor nearest the estimated center of the vortex. The core diameter can be calculated by multiplying the time separation of the twin peaks which are characteristic of core penetration by the wind velocity. In the cases shown, the estimated values are consistent with those inferred from the profile measurements. A clue to the reason for the large cores in these vortices may be found in the geometry of the aircraft. It is noted that the outboard engine exhausts only about ten feet laterally inboard of the expected center of roll-up for the flap vortex. This fact, coupled with the engine's underslung position, suggests that axial momentum and turbulence from the engine exhaust may contribute to core formation during the roll-up process. It should be emphasized, however, that with the exception of the core region, the velocity profiles for these flapped cases can be computed quite adequately with the inviscid method described earlier. The good agreement between theory and measurement also supports the contention that for wakes such as these, the stronger of the two vortices—in this case, the flap vortex—is the one which predominates. For the C-141 tests, the wind conditions were such that relatively short elapsed times were possible, the oldest vortex of those presented here being only 20 sec. This short interval is apparently insufficient to permit any measurable aging to take place.

V. Conclusions

The conclusions which may be drawn from this study are as follows:

1) The initial tangential velocity profiles in the vortex wakes of DC-7, DC-9, and C-141 aircraft can be computed with reasonable accuracy by means of the Betz roll-up theory³ as modified according to the method described in this paper. This method appears to work equally well for unflapped wings in which a single vortex concentration is found behind each half of the wing and for flapped wings in which there may be initially at least two such concentrations. The agreement between computed and measured profiles was found, within the experimental accuracy, to be independent of the age of the vortices for times as long as 62 sec, as in the case of the DC-7 in takeoff configuration. Because of the consistently observed agreement for a variety of aircraft in a variety of flight configurations, it is concluded that the primary processes which determine the roll-up and early history of wake vortices are inviscid.

2) The computed profiles for flap vortices, in general, appear to have higher velocities at moderate and large radii than do tip vortices of the same strength. This difference in circulation distribution is a direct consequence of the different wing loading distributions for the two cases. Furthermore, it has been shown that the maximum tangential velocity to be expected at the center of any inviscid Betz-type vortex is, simply, $(1/\pi) (d\Gamma/dy)_P$ where P is the point of initial roll-up for that vortex. On this basis, it is concluded that the main reason for the difference between measured profiles for aircraft with and without flaps is the alteration to the load distribution caused by the flaps and not the introduction of turbulence or other disturbances.

3) Because of the inviscid character of these wake vortices, it may be concluded that turbulence and its diffusion have little to do with determining the initial velocity profiles except, perhaps, in regions where there is a possibility for entrainment of axial momentum. In the present study, the DC-9 clean-wing design might be expected to offer little chance for such entrainment. It is not too surprising, therefore, to find that the vortex cores for this air-

craft are apparently quite small, and that there is no real evidence of aging that might be attributed to the diffusion of turbulence. The DC-7, and C-141, however, with their wing-mounted engines, present a different possibility. In the case of the DC-7, of course, because of the large sensor spacing, the resolution of detail near the center of the vortex is poor. However, the examination of the time histories of sensors near the center and the relative number of core penetrations for the three flight configurations indicate that the vortices for the flaps-down cases have both larger cores and broader profiles than do the flaps-up cases. It has been demonstrated that the latter effect can be accounted for by the change in load distribution on the wing. The former effect, however, could involve interaction with the slipstream of the outboard engine. It should be noted that with the flaps lowered, the flap vortex, which now predominates, rolls up at a point considerably inboard of the location of the unflapped wing roll-up and much closer to the engine centerline.

The C-141 data show considerable detail in support of the above interpretation. With no flaps, high-peak tangential velocities were measured which match very closely the inviscid profile at points very near the centerline. The core was quite small. With flaps extended, however, very large cores are measured. Outside of these cores, the computed inviscid profile of the flap vortex is closely matched, while inside it appears that strong viscous action is present. Because of the proximity of the center of roll-up to the engine centerline, it is reasonable to conclude that entrained axial momentum plays a part in determining the size and shape of these cores.

References

¹Spreiter, J. R. and Sacks, A. H., "The Rolling Up of the Trailing Vortex Sheet and its Effect on the Downwash Behind Wings," *Journal of the Aeronautical Sciences*, Vol. 18, No. 1, Jan. 1951, pp. 21-32.

²Donaldson, C. duP., "A Brief Review of the Aircraft Trailing Vortex Problem," presented at the National Aerospace Electronics Conference (NAECON), Dayton, Ohio, 1971; also ARAP. Rept. 155, Aeronautical Research Associates of Princeton, Princeton, N.J.

³Betz, A., "Behavior of Vortex Systems," *Zeitschrift für angewandte Mathematik und Mechanik*, Vol. 12, No. 3, June 1932; also TM 713, June 1933, NACA.

⁴Kaden, H., "Aufwicklung einer unstabilen Unstetigkeitsfläche," *Ingenieur Archiv. Bd. II*, 1931, pp. 140-168.

⁵Westwater, F. L., "Rolling Up of the Surface of Discontinuity Behind an Aerofoil of Finite Span," R&M 1962, 1935, Aeronautical Research Council, London, England.

⁶Hackett, J. E. and Evans, M. R., "Vortex Wakes Behind High-Lift Wings," *Journal of Aircraft*, Vol. 8, No. 5, May 1971, pp. 334-340.

⁷Brown, C. E., "Aerodynamics of Wake Vortices," *AIAA Journal*, Vol. 11, No. 4, April 1973, pp. 531-536.

⁸Mason, W. H. and Marchman, J. F. III, "Farfield Structure of an Aircraft Trailing Vortex, Including Effects of Mass Injection," CR-62078, April 1972, NASA.

⁹Rossov, V., "On the Inviscid Rolled-Up Structure of Lift-Generated Vortices," *Journal of Aircraft*, Vol. 10, No. 11, Nov. 1973, pp. 647-650.

¹⁰Jordan, P. F., "Structure of Betz Vortex Cores," *Journal of Aircraft*, Vol. 10, No. 11, Nov. 1973, pp. 691-693.

¹¹Yates, J. E., "Calculation of Initial Vortex Roll-Up in Aircraft Wakes," ARAP. Rept. 202, Oct. 1973, Aeronautical Research Associates of Princeton, Inc., Princeton, N.J.

¹²Bilanin, A. J., "An Analytic and Experimental Investigation of the Wakes Behind Flapped and Unflapped Wings," ARAP. Rept. 217, June 1974, Aeronautical Research Associates of Princeton, Inc., Princeton, N.J.

¹³Garodz, L. J., "Federal Aviation Administration Full-Scale Aircraft Vortex Wake Turbulence Flight Test Investigations: Past, Present, Future," AIAA Paper 71-97, New York, 1971.

¹⁴Donaldson, C. duP., Snedeker, R. S., and Sullivan, R. D., "Calculation of the Wakes of Three Transport Aircraft in Holding, Takeoff, and Landing Configurations and Comparison with Experimental Measurements," Federal Aviation Administration Rept. FAA-RD-73-42, March 1973; also Rept. 190, Aeronautical Research Associates of Princeton, Inc., Princeton, N.J.